CHAPTER 6

FIBRONECTIN INTERACTIONS WITH *STAPHYLOCOCCUS AUREUS* WITH AND WITHOUT FIBRONECTIN-BINDING PROTEINS AND THEIR ROLE IN ADHESION AND DESORPTION

Xu, C.-P., Boks, N.P., De Vries, J., Kaper, H.J., Norde, W., Busscher, H.J. and Van der Mei, H.C. (2008), *Applied and Environmental Microbiology* (in press).

Abstract

Adhesion and residence-time dependent desorption of two *Staphylococcus aureus* strains with and without fibronectin binding proteins (FnBPs) on Fn-coated glass were compared in a parallel plate flow chamber. To gain a better understanding of the role of Fn-FnBP binding, adsorption enthalpies of Fn to staphylococcal cell surfaces were determined using isothermal titration calorimetry (ITC). Interaction forces between staphylococci and Fn-coatings were measured using atomic force microscopy (AFM). The strain with FnBPs adhered faster and initially stronger to a Fn-coating than the strain without FnBPs and its Fn-adsorption enthalpies were higher. Initial desorption was high for both strains, but decreased strongly within 2 s. These time scales of staphylococcal bond ageing were confirmed by AFM adhesion force measurements. After exposure of either Fn-coating or staphylococcal cell surfaces to bovine serum albumin (BSA), adhesion of both strains to Fn-coatings was reduced, suggesting that BSA not only suppresses non-specific, but also specific Fn-FnBPs interactions. Adhesion forces and adsorption enthalpies were only slightly affected by BSA adsorption. This implies that under the mild contact conditions of convective-diffusion in the flow chamber, adsorbed BSA prevents specific interactions, but does allow forced Fn-FnBPs binding during AFM or stirring in ITC. Bond strength energies calculated from retract force-distance curves in AFM were orders of magnitude larger than from desorption data, confirming that the penetrating Fn-coated AFM tip probes multiple adhesins in the outermost cell surface that remain hidden during mild landing of an organism on a Fn-coated substratum as during convective-diffusional flow.

Introduction

Staphylococcus aureus is an extremely versatile pathogen, which can adhere to epithelial cells, endothelial cells, fibroblasts as well as to plasma exposed biomaterials implant surfaces in the human body [1], causing potentially persistent infections. The best described mechanism of *S. aureus* adhesion to eukaryotic cells and other fibronectin-coated surfaces involves the fibronectin (Fn) binding proteins FnBP A and FnBP B on the surface of *S. aureus* [2,3]. Peacock *et al*. [4] demonstrated the significant role played by the FnBPs by comparing adhesion of different isogenic *S. aureus* strains to human endothelial cells. Moreover, *in vitro* adhesion of *S. aureus* strain Wood 46 to Fn-coated surfaces was demonstrated to be inhibited in a dose-dependent manner by anti-Fn antibodies [5,6].

At constant temperature and pressure, which is usually the case in biological systems, all physico-chemical interactions, including adsorption, (co-) adhesion and (co-)aggregation, are determined by changes in the Gibbs energy (G) of a system. These interactions can either be evaluated at a macroscopic level, in terms of Lifshitz-Van der Waals, electrostatic and hydrophobic forces originating from overall characteristics of bacteria and substrata, or at a more microscopic or even nanoscopic level, where highly specific interactions between stereo-chemical surface components, such as fibronectin and FnBPs are considered. For a spontaneous process, the change in Gibbs energy (ΔG) is negative. ΔG is composed of a change in enthalpy (ΔH) and in entropy (ΔS), according to

$$\Delta G = \Delta H - T\ \Delta S \qquad (1)$$

where T is the temperature in Kelvin. The enthalpy tends to reach a minimum value, whereas the entropy strives for a maximum. The enthalpy of a system is

directly related to its heat content. At constant pressure, and if no work other than that related to volume change is involved, the enthalpy change can be determined as the heat exchange between a system and its environment. Direct determination of the entropy, however, is practically impossible as it would require counting all conformational and configurational possibilities before and after a process. Many biological processes are characterized by strong enthalpy-entropy compensation [7], that is, they occur spontaneously by virtue of an entropy increase that compensates for an unfavourable enthalpy effect, or vice versa. The enthalpy of interaction between bacterial cell surfaces and proteins can be assessed using isothermal titration calorimetry (ITC). ITC measures the enthalpy change of formation of a complex at constant temperature. Xu *et al.* [8] determined the adsorption enthalpies of salivary proteins to *Streptococcus mutans* and found that *S. mutans* LT11 with antigen I/II, a cell surface binding protein involved in bacterial adhesion to extracellular matrix proteins, yielded a much higher, exothermic adsorption enthalpy when mixed with saliva at pH 6.8 than did *S. mutans* IB03987, lacking surface antigen I/II. It was thus inferred that antigen I/II at the surface of *S. mutans* LT11 specifically binds different proteins with different affinities from the large pool of proteins present in whole saliva. Furthermore, Busscher *et al.* [9] used ITC to evaluate the adsorption of a single protein, laminin, to these streptococcal cell surfaces and found that enthalpy is released upon adsorption of laminin to the surface of the parent strain LT11, but not upon adsorption to IB03987. Whereas ITC operates at a macroscopic level, atomic force microscopy (AFM) senses at the nanometer level and allows to determine the force between a sharp probe attached to a flexible cantilever and a cell surface and can thus distinguish between different functional surface proteins [10]. Using AFM, differences in interaction forces between protein-coated AFM probes and streptococcal strains with and without antigen I/II have been measured. Generally, upon retraction of streptococci from

saliva- or laminin-coated probes, stronger forces were observed when the streptococcal strain possessed antigen I/II than when it did not.

Initial microbial adhesion is reversible, but over time the bond strength may increase and adhesion becomes less reversible. The kinetics of microbial adhesion and desorption can be investigated simultaneously in a parallel plate flow chamber with *in situ* observation and real-time image analysis. Moreover, by registering the time of arrival and detachment of an adhering microorganism, desorption can be measured as a function of the residence time of an adhering organism [11-13]. Dabros and Van de Ven [11] proposed that the desorption rate coefficient of a particle adsorbed at time τ and desorbing at time t, *i.e.* after residing on the surface for a time $(t-\tau)$, changes exponentially from an initial value β_0 to a final value β_∞ during ageing of the bond with a relaxation time $1/\delta$ according to:

$$\beta(t-\tau) = \beta_\infty-(\beta_\infty-\beta_0)e^{-\delta(t-\tau)} \qquad (2)$$

Meinders *et al.* [14] applied this equation to analyze the residence time-dependent desorption of *Streptococcus thermophilus* B during non-specific adhesion on glass, and found that the desorption rate coefficient decreased according to Eq. (2) from an initially high value β_0 (2.5×10^{-3} s^{-1}) to an almost negligibly low value β_∞ (0.01×10^{-3} s^{-1}) over a time scale of approximately 50 s. Many years later, atomic force microscopy (AFM) was applied to directly measure the strengthening of the adhesion force between *S. thermophilus* B and a silicon nitride (Si_3Ni_4) AFM tip and bond strengthening by a factor of 2 to 3 was found to occur over a similar time scale as the residence-time dependent desorption [15]. However, *S. thermophilus* B adheres to glass utilizing non-specific adhesion mechanisms, which are very different from the specific mechanisms applied by *S. aureus* strains in their adhesion to Fn-films.

Therefore, the aim of this study is to analyze the role of FnBPs on *S. aureus* cell surfaces in their interaction with (adsorbed) Fn using ITC and AFM,

in particular in relation to adhesion and residence-time dependent desorption on Fn-coated surfaces under flow. To this end, we first determined adhesion and desorption of a *S. aureus* wild type strain 8325-4 and of an isogenic mutant DU5883 lacking FnBPs, deposited by convective-diffusion on Fn-coated glass slides in a parallel plate flow chamber. Subsequently, interaction forces between Fn-coated AFM tips and the cell surfaces were compared, while furthermore the enthalpies of adsorption of Fn to the surfaces of the *S. aureus* strains were measured. In order to determine to what extent Fn-binding to *S. aureus* cell surfaces is dominated by specific interactions, additional experiments were performed after coating either the substrata or the staphylococcal cells with a layer of bovine serum albumin (BSA).

Materials and Methods

Bacterial strains and culture conditions. *S. aureus* strain 8325-4 and its isogenic mutant lacking FnBPs, DU5883 (kindly provided by Dr. T.J. Foster, Moyne Institute of Preventive Medicine, Dublin, Ireland), were used in this study. The bacterial cells were maintained at -80^{o}C in tryptone soya broth (TSB; OXOID, Basingstoke, UK) containing 7% dimethylsulfoxide (DMSO; MERCK, Germany). For culturing, both strains were plated onto TSB agar plates overnight at 37^{o}C. Subsequently, bacterial colonies were precultured in 10 ml TSB batch culture overnight under constant rotation. This preculture was used to inoculate a main culture of 190 ml TSB. After approximately 2 h of growth to early stationary phase, corresponding with peak expression of FnBPs in *S. aureus* 8325-4 [16], bacteria were harvested by centrifugation at 6500g for 5 min at 10^{o}C and washed twice with demineralised water. Bacterial chains and aggregates were broken by mild sonication on ice for 3 × 10 s at 30 W (Vibra Cell model 375, Sonics and Materials Inc., Danbury, Connecticut, USA). Then

bacteria were resuspended in phosphate-buffered saline (PBS; 10 mM potassium phosphate and 0.15 M NaCl, pH 7), to a concentration of 3×10^8 or 5×10^9 per ml for adhesion experiments or ITC, respectively, as determined in a Bürker-Türk counting chamber. In order to block FnBPs on the staphylococcal cell surfaces, staphylococci were also incubated for 60 min at 37°C in PBS supplemented with 1% BSA.

Bacterial deposition to a Fn-film in a parallel plate flow chamber. The deposition experiments were carried out in a parallel plate flow chamber (internal dimensions: length × width × height, 175 × 17 × 0.75 mm) equipped with image analysis options [17]. The bottom glass plate (76 × 26 mm) of the flow chamber was first cleaned by sonication for 3 min in a surfactant solution (2 % RBS 35 detergent in water; Omniclean), rinsed thoroughly with tap water, and then washed with methanol, thoroughly rinsed with tap water and finally with demineralised water. Subsequently, the centre of the glass plate was drop-coated with 0.05 ml Fn (25 μg ml^{-1} human Fn, Sigma-Aldrich BV, Zwijndrecht, The Netherlands) for 2 h at room temperature to create a circular Fn-coated region with a diameter of approximately 1 cm on which staphylococcal adhesion was monitored. In addition, glass plates were prepared on which non-specific adhesion sites were blocked by immersing the entire glass plate, including the Fn-coated region for 1 min in PBS containing 1% BSA. Glass plates were rinsed after protein coating with demineralised water. Bacterial adhesion was monitored with a phase-contrast microscope (Olympus BH-2) equipped with a ×40 ultra-long-working-distance lens (Olympus ULWD-CD plan 40 PL) and coupled to a Firewire CCD camera (Basler AG, Germany).

The flow rate during the experiments was adjusted to 1.4 ml min^{-1} under the influence of a hydrostatic pressure yielding a shear rate of 15 s^{-1}. During flow experiments, 15 images (1392 × 1040 pixels) were grabbed every second. These 15 frames were averaged on a pixel by pixel basis in order to distinguish

between adhered and in focus moving bacteria. The averaged frame was computer-stored for subsequent offline analysis using proprietary software based on the Matlab Image Processing Toolkit (The Mathworks, MA, USA). Further analysis consisted of locating the staphylococci on the substratum surface and comparison of their positions in a current image with their positions in previous images to determine the total number of adhering bacteria $n(t)$ as a function of time during 4 h as well as their residence times. The affinity of an organism for the Fn-coated glass surface was expressed as the initial deposition rate j_0, representing the initial increase of $n(t)$ with time. Note that since the initial deposition rate is derived only from the first adhering bacteria, it represents the affinity of the organisms for the adsorbed Fn-coatings without intervening influences of interactions between adhering bacteria, as occurs due to crowding at the surface, such as after 4 h [17]. Finally, the staphylococcal desorption rate coefficient $\beta(t-\tau)$ as a function of residence-time $(t-\tau)$ was calculated according to [14]:

$$\beta(t-\tau) = \sum_{j=1}^{N-1} \frac{1}{N-j-1} \sum_{i=j+1}^{N} \frac{\Delta n_{des}(t_i)}{\Delta n_{ads}(\tau_{i-j})(t_i - t_{i-1})} \qquad (3)$$

where the summation runs over the number of images taken, $\Delta n_{\mathrm{des}}(t_i)$ is the number of bacterial desorbing between time $t_{\mathrm{i\text{-}1}}$ and t_i and adsorbing between time $\tau_{i\text{-}j\text{-}1}$ and $\tau_{i\text{-}j}$, and $\Delta n_{\mathrm{ads}}(t_{i\text{-}j})$ is the total number of adsorbed bacteria between time $\tau_{i\text{-}j\text{-}1}$ and $\tau_{i\text{-}j}$. The residence–time dependent desorption rates calculated were fitted to Eq. (2) to yield the initial and final desorption rate coefficients (β_0 and β_∞, respectively) and their relaxation time $1/\delta$.

All adhesion and desorption experiments in the parallel plate flow chamber were done in four-fold with separate bacterial cultures.

Atomic force microscopy. For AFM, the negatively charged bacteria were attached through electrostatic interactions to a glass slide, made positively

charged through pre-adsorption of poly-L-lysine, as described before [18]. AFM tips (DNP from Veeco, Woodbury, USA) were coated with a Fn-film by immersion for 30 min in a Fn-solution (25 μg ml^{-1} in PBS, pH 7) with the aid of a micromanipulator. All glass slides with immobilized bacteria and Fn-coated AFM tips were immediately used after preparation. To block non-specific binding sites on the bacterial cell surfaces, the glass slides with attached bacteria were also immersed for 1 min in PBS containing 1% BSA and rinsed with demineralised water.

AFM measurements were done at room temperature in PBS using a Dimension 3100 system (Nanoscope IV Digital Instrument, Woodbury, USA). Nanoscope imaging software (version 6.13r1, Veeco) was used to analyze the resulting images. All AFM cantilevers were calibrated using resonant frequency measurements [19] and the slopes of the retract force curves, in the region where probe and sample are in contact, were used to translate the voltage into cantilever deflection. Force-distance curves were generated and approach curves analyzed for the repulsive force at contact. Retraction of the tip from the bacterial surface was carried out after 0 and 2 s contact time between the AFM tip and staphylococcal cell surface to demonstrate strengthening of the adhesion force. Retract curves were integrated to yield the bond strength energy for the two surface delay times evaluated.

Three different bacterial cells were examined at ten locations for each particular case, yielding 30 force-distance curves. This resulted in a non-parametric distribution, from which median, mode and range values were derived.

Isothermal titration calorimetry. The adsorption enthalpy of Fn to the bacterial cell surfaces was measured in a twin-type, isothermal microcalorimeter TAM 2277 (Thermometric, Sweden). The calorimeter was positioned in a

temperature-controlled environment (20 ± 0.1°C), allowing a baseline stability of ± 0.1 μW over 24 h [20]. The instrument had an electrical calibration with a precision better than 1% and proper calibration was regularly checked by measuring the dilution enthalpy of concentrated sucrose solutions [21]. Experiments were performed isothermally at 25°C in stainless steel ampoules of 4 ml. Four ampoules, connected with separate titration systems, were used inside the microcalorimeter. The use of a twin-type microcalorimeter allows the measurement of the heat (Q) flowing from the reaction ampoule as compared with a reference ampoule. The output signal was collected as power, P, versus time, t, and was integrated to evaluate the isobaric heat exchange (the enthalpy change) during adsorption, using the dedicated Digitam 4.1 software (Thermometric, Sweden). Notably, the measured heat effect should be corrected for the heat of dilution of the proteins to obtain the net adsorption enthalpy [22].

Typically, all four reaction ampoules including the reference ampoule, were filled with 1.5 ml of bacterial suspension (5 $\times 10^9$ cells per ml) in PBS under constant stirring (90 rpm) with a specially designed two-blades stirrer. The ampoules were lowered gradually into the microcalorimeter and left in the measuring position to reach thermal equilibrium before data collection started. After equilibration, a stable baseline was obtained and Fn was titrated into the reaction ampoules. Titration was done at a controlled rate of 2 μl s^{-1} via a stainless steel cannula connected to a syringe. In order to study possible saturation of adsorption sites, Fn solution (25 μg ml^{-1}) was added in four consecutive injections of 60 μl into the ampoule with intervals of 40 min. All calorimetric experiments were done in fourfold.

Statistical analysis. Data were analyzed with the statistical package for the social sciences (Version 11.0, SPSS, Chicago, Illinois, USA). Median values of the repulsive force at contact (F_0) upon approach, the adhesion force (F_{adh}) upon

retract, as well as of the bond strength energy were analyzed using the Wilcoxon signed rank test for the median. A Student's t-test was used to determine significant differences in initial deposition rates, adhesion numbers after 4 h, initial and final desorption rate coefficients, and their relaxation time as well as in interaction enthalpies. The level of significance was set at $p < 0.05$.

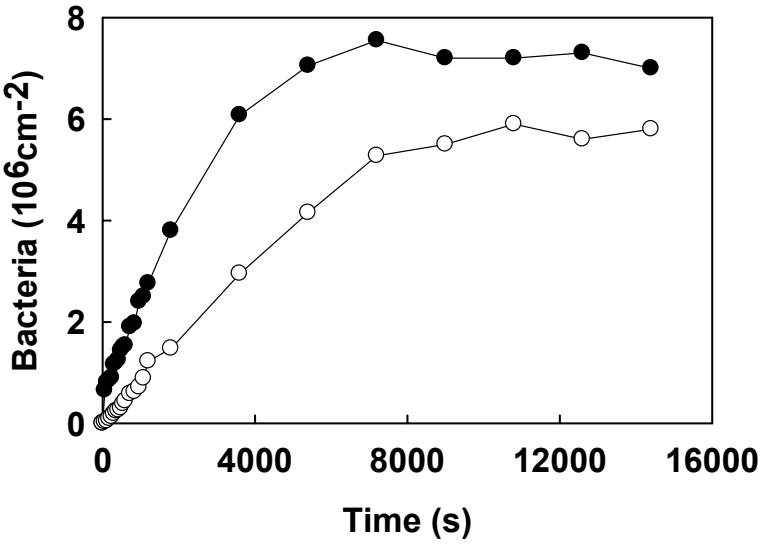

Figure 1. Representative examples of the adhesion kinetics of *S. aureus* 8325-4 (●) and DU5883 (○) to Fn-films in PBS.

Results

Adhesion and residence time dependent desorption of *S. aureus* from Fn-films. Figure 1 shows representative examples of the adhesion kinetics of *S. aureus* 8325-4 and DU5883 to Fn-coatings in a parallel plate flow chamber in PBS at pH 7. The adhesion kinetics of both *S. aureus* strains are linear during approximately 4000-5000 s prior to levelling off toward stationary numbers. The linear trajectories of the curves are taken to calculate the initial deposition rates, as summarized in Table 1. The initial deposition rate of *S. aureus* 8325-4 is about twice as high as the one of FnBPs deficient DU5883, which indicates the

Table 1. Mean values for the initial deposition rate (j_0) and numbers adhering after 4 h (n_{4h}), initial (β_0) and final desorption rate coefficients (β_∞) together with the relaxation time for bond ageing ($1/\delta$) for *S. aureus* 8325-4 with fibronectin binding proteins (FnBPs) and isogenic mutant DU5883 without FnBPs from Fn-coatings. Experiments were performed prior to and after exposure of the substrata or the staphylococci to a 1% BSA solution. Average standard deviations over four separate experiments amount ± 110 cm^{-2} s^{-1} and ± 0.5 × 10^6 cm^{-2} over the initial deposition rates and numbers of bacteria adhering after 4 h, respectively; ± 124 x 10^{-3} s^{-1} and ± 0.3 x 10^{-3} s^{-1} over the initial and final desorption rate coefficients, respectively, and ± 0.3 s in the relaxation time for bond ageing.

Substratum	j_0 (cm^{-2} s^{-1})		n_{4h} (10^6 cm^{-2})		β_0 (10^{-3} s^{-1})		β_∞ (10^{-3} s^{-1})		$1/\delta$ (s)	
	8325-4	**DU5883**	**8325-4**	**DU5883**	**8325-4**	**DU5883**	**8325-4**	**DU5883**	**8325-4**	**DU5883**
Fn-coated glass	2438	1290	7.0	5.2	307	463	1.0	1.2	0.9	0.9
Fn and BSA-coated glass	815	678	5.2	4.4	200	170	0.6	0.4	1.0	1.2
Fn-coated glass*	704	527	3.9	3.5	334	504	0.6	1.8	0.9	0.9

* These experiments were carried out with staphylococci exposed to 1% BSA prior to the experiments

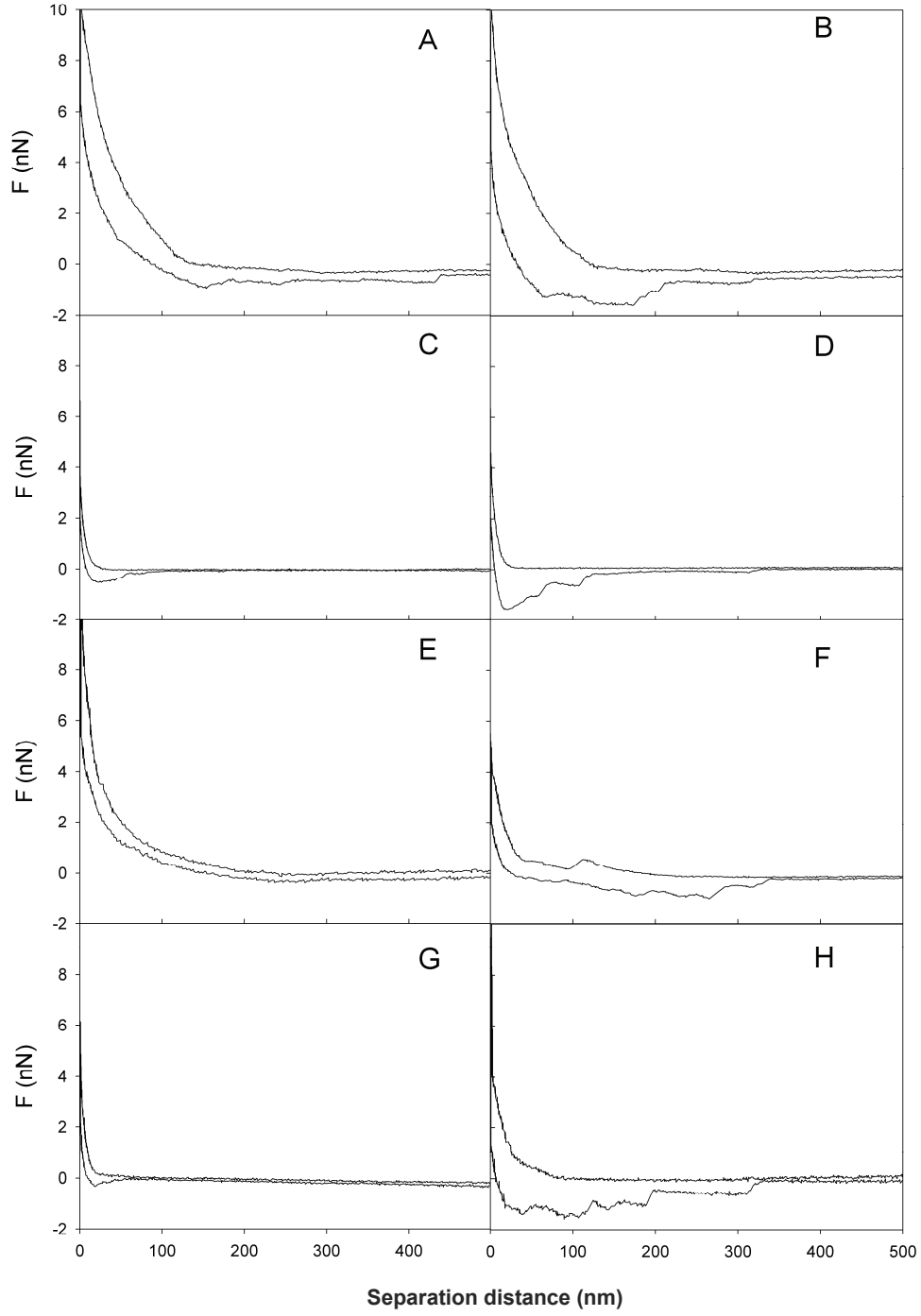

Figure 2. Representative examples of force-distance curve between an Fn-coated AFM tip and staphylococcal cell surfaces: *S. aureus* 8325-4 after 0 s surface delay (A), *S. aureus* 8325-4 after 2 s surface delay (B), *S. aureus* DU5883 after 0 s surface delay (C), *S. aureus* DU5883 after 2 s surface delay (D), *S. aureus* 8325-4 coated with BSA after 0 s surface delay (E), *S. aureus* 8325-4 coated with BSA after 2 s surface delay (F), *S. aureus* DU5883 coated with BSA after 0 s surface delay (G) and S. *aureus* DU5883 coated with BSA after 2 s surface delay (H).

relatively high affinity of strain 8325-4 for Fn-coatings. Also after 4 h of deposition, strain 8325-4 adheres in higher numbers than FnBPs deficient DU5883, but the difference is not two-fold anymore as in initial deposition rates. After exposure of either the Fn-coating or the staphylococci to BSA, initial deposition rates and the numbers of bacteria adhering after 4 h decreased significantly for both strains.

Table 1 also summarizes desorption characteristics of the two staphylococcal strains. Exposure of either the Fn-coated surface or the bacterial cells to BSA has only a minor effect, if any, on the initial desorption rate coefficients (β_0), which suggests that the desorbing bacteria mainly leave non-specific binding sites. Desorption rates decrease with increasing residence-times for both strains, regardless of the absence or presence of a BSA-coating on the surfaces with relaxation times for bond ageing less than 2 s. Final desorption rate coefficients (β_∞) are similar for both strains without significant influences of bacterial exposure to BSA and with a slight reduction in final desorption rates after exposure of the Fn-coated surface to BSA.

Bond strengthening between Fn-coatings and *S. aureus* cell surfaces. Median values of the interaction forces measured using AFM are summarized in Table 2. The repulsive force at contact F_0, is significantly ($p < 0.05$) stronger for *S. aureus* 8325-4 with FnBPs than for *S. aureus* DU5883. Blocking of non-specific binding sites on the staphylococcal cell surfaces has little (*S. aureus* DU5883) or no (*S. aureus* 8325-4) influence on the repulsive force upon approach. However, upon retract, median adhesion forces were significantly stronger after a 2 s surface delay than when measured immediately, *i.e.* with a 0 s surface delay. There is no significant difference in adhesion forces between the two strains. Interestingly, the distance over which the adhesion forces are operative varies considerably between the different conditions applied, (see Fig. 2) which translates in significant differences in bond strength energies. Initial

Table 2. Median values[1)] for the repulsive forces at contact F_0 upon approach[2)], adhesion force F_{adh} upon retract and associated bond strength energies for the interaction between Fn-coated AFM tips and *S. aureus* 8325-4 and an isogenic mutant without FnBPs, DU5883 prior to and after bacterial exposure to 1% BSA. All experiments were done in three-fold with separately prepared Fn-coated AFM tips and different bacterial cultures, yielding thirty force-distance curves.

Delay time (s)	Treatment	Repulsive force at contact F_0 (nN)		Adhesion force F_{adh} (nN)		Bond strength energy (10^{-16}J)	
		8325-4	DU5883	8325-4	DU5883	8325-4	DU5883
0	**No BSA**	9.1	6.0	-0.7	-0.6	-98	-32
	1% BSA	9.0	3.9	-0.6	-0.5	-64	-21
2	**No BSA**	9.1	6.0	-1.5	-1.7	-187	-181
	1% BSA	9.0	3.9	-1.1	-1.1	-176	-149

[1)] distribution functions were made taking a class width of 0.1 nN.

[2)] these data comprise repulsive forces at contact measured in experiments with and without a surface delay and thus refer to 30 force-distance curves.

bond strength energies of *S. aureus* 8325-4 with FnBPs are significantly ($p < 0.05$) higher than for *S. aureus* DU5883 without FnBPs, regardless of exposure of the staphylococci to a 1% BSA solution. Both strains show a significant increase in bond strength energy by a factor 2 to 3 when the surface delay time is increased from 0 to 2 s for *S. aureus* 8325-4 and even more (factor 4 to 5) for *S. aureus* DU5883 (Table 2). Furthermore, after a surface delay, effects of BSA exposure of the staphylococci on bond strength energies disappear.

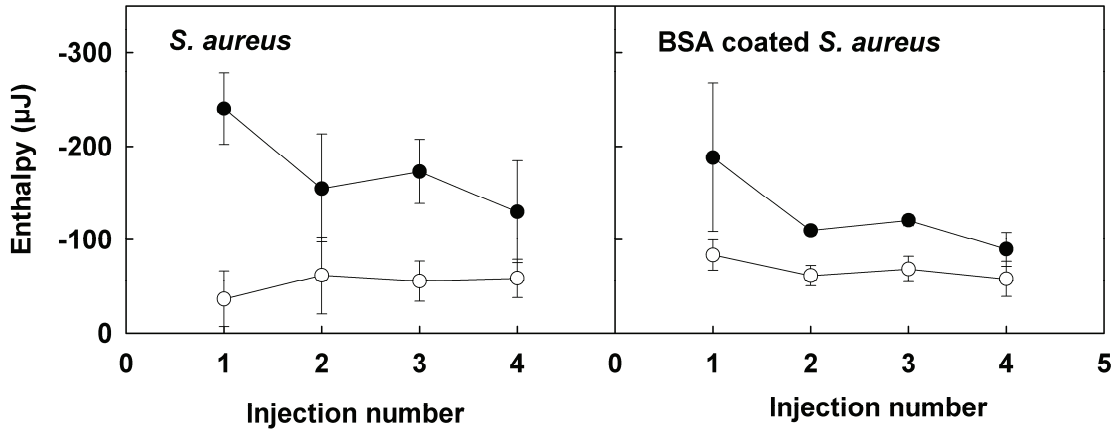

Figure 3. Adsorption enthalpies (μJ), after correction for dilution effects, of Fn to *S. aureus* cell surfaces upon consecutive injections of 60 μl Fn solution (25 μg/ml) into 1.5 ml bacterial suspension of *S. aureus* 8325-4 (●) and *S. aureus* DU5883 (○) in PBS. Right panel data refer to staphylococci first exposed to 1% BSA. Error bars indicate standard deviation based on four independent measurements.

Enthalpies of adsorption of Fn to *S. aureus* cell surface. The measurement of adsorption enthalpies of Fn to the *S. aureus* cell surfaces requires correction for the heat of diluting of the proteins in PBS. For four consecutive injections of 60 μl of a 25 μg ml^{-1} Fn-solution into 1.5 ml of PBS yielded heat effects of, respectively, -55, -56, -37 and -37 × 10^{-9} μJ. Figure 3 summarizes the adsorption enthalpies upon consecutive injections of Fn to the staphylococcal suspensions, after correction for protein dilution. For the parent strain 8325-4 with FnBPs adsorption enthalpies decrease with the number of injections done, but no saturation of adsorption sites seems to be reached within four injections. For

strain DU5883 the enthalpy effects are essentially invariant with the number of injections. The cumulative adsorption enthalpies after the four injections are shown in Table 3, as expressed per bacterium and per m^2 bacterial cell surface. Fn adsorption to the bacterial cell surfaces is an exothermic process in all cases, *i.e.* enthalpy is released upon adsorption. Adsorption of Fn to *S. aureus* 8325-4 with FnBPs is enthalpically significantly more favourable than to *S. aureus* DU5883. After exposure to BSA of *S. aureus* 8325-4, the adsorption enthalpy decreases significantly, but remains larger than those for *S. aureus* DU5883. No significant effect is seen for exposure to BSA on the adsorption enthalpy of *S. aureus* DU5883, lacking FnBPs.

Table 3. Cumulative adsorption enthalpies per bacterium (10^{-9}μJ) and per m^2 bacterial cell surface (mJ m^{-2}) after four consecutive injections of 60 μl Fn solution (25 μg ml^{-1}) into 1.5 ml bacterial suspensions in PBS. Average standard deviations over 4 separate experiments amount ± 25 × 10^{-9} μJ per bacterium and ± 8 mJ m^{-2}, respectively.

Experiments	**Cumulative adsorption enthalpies per bacterium (10^{-9}μJ)**		**Cumulative adsorption enthalpies per m^2 (mJ)**	
	8325-4	**DU5883**	**8325-4**	**DU5883**
No BSA	-140	-43	-44	-14
1% BSA	-102	-54	-32	-17

* for calculation of the adsorption enthalpies per m^2, it was assumed that the bacterial cell radius was 0.5 μm.

Discussion

In this chapter, we compare the interactions mediating adhesion to Fn-coated surfaces as well as desorption of two *S. aureus* strains, one containing FnBPs and the other one being FnBP-deficient, using three entirely different techniques. Adhesion and residence-time dependent desorption of the two

strains is determined in a parallel plate flow chamber under convective-diffusion. In addition, the adhesion forces to Fn-coated AFM tips were measured as well as the adsorption enthalpies of Fn to the staphylococcal cell surfaces. In general, adhesion of the strain with FnBPs to Fn-coated substrata occurs faster and in higher numbers than that of the strain deficient of FnBPs and, in line, adhesive bonds are stronger and adsorption enthalpies higher. Surprisingly, adsorption of BSA to either the Fn-coated substrata or the staphylococcal cell surfaces not only blocks non-specific adhesion/adsorption sites, but also obstructs the accessibility of the FnBPs on strain 8325-4 during convective-diffusional mass transport, as, in this case, adhesion approaches that of the FnBP-deficient strain DU5883. Influences of a BSA-coating on interaction forces and adsorption enthalpies are far less significant, however. Strengthening of the bond is evident from the resident-time dependent desorption of both strains as measured in a parallel plate flow chamber as well as from a comparison of the adhesion forces and adhesive bond strength energies measured after 0 and 2 s surface delays in AFM.

Adsorption enthalpies. The enthalpy changes associated with the interaction between Fn and the *S. aureus* cells are all exothermic, but differ markedly between the two strains, as shown in Fig. 3 and Table 3. For the FnBP-deficient DU5883 strain the enthalpy change is essentially the same for each injection step, as is to be expected for non-specific adsorption in the sub-saturation range. Assuming that the staphylococcal cell diameter equals 1 μm, it can be calculated that in the ITC ampoule there is 23.6×10^{-3} m^2 of bacterial surface area available for adsorption. Since each fibronectin injection adds 1.5×10^{-3} mg Fn, the maximal cell surface coverage by fibronectin after 4 consecutive injections amounts 0.25 mg Fn per m^2 bacterial cell surface, which is far below the saturation limit for non-specifically adsorbed Fn, which would amount to at least

a few mg m^{-2} [23]. Assuming that all Fn added is adsorbed, the cumulative enthalpy effect measured of -14 mJ m^{-2} corresponds to -13.8×10^3 kJ per mol Fn (which corresponds to about 5600 *kT* per molecule Fn at 25°C), as calculated using a molar mass of 250 kDa. Taking into account the large molar mass of Fn, this value is quite reasonable when compared with enthalpy effects reported for non-specific adsorption of various proteins to different surfaces [24]. The enthalpy effects measured for the FnBPs containing strain 8325-4 are more exothermic than for the FnBP-deficient strain DU5883. This indicates involvement of enthalpically favourable specific Fn-binding sites. The downward trend of the interaction enthalpy with consecutive injection steps, displayed in Fig. 3 (left panel), suggests that not all specific binding sites are equally favourable, or, alternatively, that they become gradually saturated, so that for each subsequent addition a smaller fraction of Fn binds to FnBPs on the cell surface. Assuming that all Fn added during the first injection binds to FnBPs, the measured -250 μJ corresponds to -41.7×10^3 kJ per mol Fn. This is about 300× higher than the enthalpy of the biotin-streptavidin interaction [25]. However, it should be realized that the much larger Fn molecule may interact through more binding sites than the number of sites involved in e.g. a single biotin-streptavidin interaction.

Exposure of the bacteria to a BSA solution hardly influences the enthalpy of interaction between Fn and the FnBP-deficient strain DU5883. In contrast, BSA exposure of the FnBP-containing strain 8325-4 significantly suppresses the enthalpy of interaction with Fn, but not even nearly to the level of a non-specific interaction. However, the downward trend in enthalpy for the BSA-coated strain 8325-4 (Fig. 3, right panel) seems to indicate that for the later Fn injections, smaller fractions of Fn added finds FnBPs, as compared to the non-BSA-coated cells. This is completely in line with the lack of effects of BSA coating on adhesion forces observed by AFM and attests to the forceful contact established

during AFM or stirring in the microcalorimeter as compared with the spontaneous and relatively mild nature of cell-surface interaction during convective-diffusion in the parallel plate flow chamber.

Interaction forces. AFM adhesion forces to Fn-coated surfaces are similar for both *S. aureus* strains. This is unexpected considering their different abilities to adsorb fibronectin [16]. Adsorption of fibronectin is a process occurring at the outermost cell surface. However, the Fn-coated AFM tip penetrates the cell surface therewith probing underneath the outermost cell surface. It is clear that, upon penetration, for both *S. aureus* strains FnBPs or other adhesins are encountered in the cell wall, even for strain DU5883 generally considered to be devoid of FnBPs [16]. However, the spatial distribution of adhesins in strain 8325-4 must be completely different than in strain DU5883, as its adhesion forces reach out much further and consequently strain 8325-4 has a higher Fn-bond strength energy than strain DU5883 (see Table 2). Under the conditions of convective-diffusion prevailing in the parallel plate flow chamber, it can be envisaged that bacteria land mildly at the substratum surface, therewith invoking interaction with only the outermost region of the cell wall. Contrary, the penetrating AFM tip senses similar bond strength energies with no influence of an adsorbed BSA-film over the cell surface. Mendez-Vilas et al. [26,27] has suggested that a penetrating AFM tip may cause irreversible damage to the inner cell surface, as concluded from saw-tooth patterns in the force-distance curves at close approach. As we observed no such patterns in our force-distance curves (see also Fig. 2), it is considered unlikely that the AFM tip has caused such cell surface damage. Moreover, we regularly checked whether interaction of our Fn-coated tips with clean glass yielded the same force values, and this was always the case within one series of experiments.

Residence-time dependent desorption. Desorption rate coefficients from a Fn-coated surface decrease for both *S. aureus* strains within 2 s by a factor of about 300-400. It is remarkable that the desorption rates and their residence time dependence are insensitive to whether or not specific Fn-FnBP interactions were involved in the adhesion. Apparently, the cells of strain 8325-4 that desorb belong to the fraction of the population that have not been able to adhere through strong specific bonds. Accordingly, exposure of either the bacterial cells or the Fn-coated surface to BSA, therewith blocking specific Fn-FnBP interactions has no or little effect on desorption kinetics. The decreasing desorption rate coefficients could be confirmed by independent AFM measurements.

Assuming that for a given condition, all bacteria adhere with the same bond strength, a staphylococcal bond strength energy can also be calculated from the desorption rate coefficients measured in the parallel plate flow chamber, by applying

$$\boldsymbol{\beta_{esc}} = \frac{j_0}{c\Delta h} e^{\varphi_m / kT} \qquad (4)$$

where β_{esc} is the desorption rate coefficient, j_0 the initial deposition rate, c the bacterial cell concentration at the entrance of the flow chamber, Δh the width of the energy minimum, φ_m depth of the energy minimum and kT the energy of thermal motion [14,28]. The initial bond strength energies of our staphylococcal strains to a Fn-film in the absence of a BSA-coating can be calculated from the initial desorption rate coefficients and ranges between 2.2 to 3.3 kT, which seems quite reasonable for non-specific binding. After bond ageing, the use of the final desorption rate coefficients yields much higher bond strength energies between 8.2 and 9.0 kT. Yet, these bond strength energies are orders of magnitude smaller than derived from AFM, and conversion of the bond strength energies from Table 2 to a thermal energy scale yields values of around 10^6 kT.

This huge number attests to the fact that the penetrating, Fn-coated AFM tip must have encountered numerous adhesins in the cell surface.

Conclusions

The combined use of a parallel plate flow chamber, AFM and ITC has yielded new insights in the mechanisms of interaction between adsorbed Fn-films and *S. aureus* strains, one of which (strain 8325-4) has FnBPs on its cell surface whereas the other one (strain DU5883) is generally considered to be devoid of FnBPs. First of all, the differences between the two strains with respect to (a) initial deposition rate at a Fn-coated surface, (b) strength of binding to a Fn-coated AFM tip and (c) enthalpy of interaction with Fn indicate that for 8325-4 additional attractive forces are involved which are ascribed to specific FnBP-Fn interaction. Most interestingly, exposure of either Fn-coatings or staphylococcal cell surfaces to BSA, strongly reduces staphylococcal adhesion under convective-diffusion, but their enthalpy of Fn adsorption and their adhesion force upon retracting a Fn-coated tip from the staphylococcal cell surface are much less, if at all, influenced by a BSA-coating. It suggests that AFM and calorimetry not only probe interactions at the outermost surfaces of the interacting species but also those occurring underneath the BSA coating. Residence-time dependent desorption data and AFM measurements reveal considerable bond strengthening within a few seconds of contact for both *S. aureus* strains. Bond strength energies calculated from the retract force-distance curves in AFM were orders of magnitude larger than calculated from desorption rate coefficients. This is another indication that the penetrating Fn-coated AFM tip probes multiple receptor sites in the cell surface, for *S. aureus* 8325-4 as well as DU5883. Apparently, mild landing of an organism on a Fn-coated substratum

as during convective-diffusion in the parallel plate flow chamber clearly does not invoke specific interactions with deeper located adhesins.

Acknowledgements

We like to thank ZON-MW for grant 91105005 enabling the purchase of the Nanoscope IV Digital Instrument.

References

1. **Lowy, F.D. (1998),** Medical progress - *Staphylococcus aureus* infections, *N Eng J Med* **339,** 520 - 532.

2. **Fowler, T., Wann, E.R., Joh, D., Johansson, S.A., Foster, T.J. and Hook, M. (2000),** Cellular invasion by *Staphylococcus aureus* involves a fibronectin bridge between the bacterial fibronectin-binding MSCRAMMS and host cell β1 integrins, *Eur J Cell Biol* **79,** 672 - 679.

3. **Greene, C., Mcdevitt, D., Francois, P., Vaudaux, P.E., Lew, D.P. and Foster, T.J. (1995),** Adhesion properties of mutants of *Staphylococcus aureus* defective in fibronectin-binding proteins and studies on the expression of fnb genes, *Mol Microbiol* **17,** 1143 - 1152.

4. **Peacock, S.J., Foster, T.J., Cameron, B.J. and Berendt, A.R. (1999),** Bacterial fibronectin-binding proteins and endothelial cell surface fibronectin mediate adherence of *Staphylococcus aureus* to resting human endothelial cells, *Microbiol* **145,** 3477 - 3486.

5. **Vaudaux, P., Suzuki, R., Waldvogel, F.A., Morgenthaler, J.J. and Nydegger, U.E. (1984),** Foreign-body infection - Role of fibronectin as a ligand for the adherence of *Staphylococcus aureus*, *J Infect Dis* **150,** 546 - 553.

6. **Vaudaux, P.E., Waldvogel, F.A., Morgenthaler, J.J. and Nydegger, U.E. (1984),** Adsorption of fibronectin onto polymethylmethacrylate and promotion of *Staphylococcus aureus* adherence, *Infect Immunol* **45,** 768 - 774.

7. **Haynes, C.A. and Norde, W. (1995),** Structures and stabilities of adsorbed proteins, *J Colloid Interf Sci* **169,** 313 - 328.

8. **Xu, C.P., Van de Belt-Gritter, B.V., Busscher, H.J., Van der Mei, H.C. and Norde, W. (2007),** Calorimetric comparison of the interactions between salivary proteins and *Streptococcus mutans* with and without antigen i/ii, *Colloid Surface B* **54,** 193 - 199.

9. **Busscher, H.J., Van de Belt-Gritter, B., Dijkstra, R.J.B., Norde, W., Petersen, F.C., Scheie, A.A. and Van der Mei, H.C. (2007),** Intermolecular forces and enthalpies in the adhesion of *Streptococcus mutans* and an antigen i/ii-deficient mutant to laminin films, *J Bacteriol* **189,** 2988 - 2995.

10. **Binnig, G., Quate, C.F. and Gerber, C. (1986),** Atomic force microscope, *Phys Rev Lett* **56,** 930 - 933.

11. **Dabros, T. and van de Ven, T.G.M. (1982),** Kinetics of coating by colloidal particles, *J Colloid Interf Sci* **89,** 232 - 244.

12. **Sjollema, J., Van der Mei, H.C., Uyen, H.M. and Busscher, H.J. (1990),** Direct observations of cooperative effects in oral streptococcal adhesion to glass by analysis of the spatial arrangement of adhering bacteria, *FEMS Microbiol Let* **69,** 263 - 269.

13. **Van de Ven, T.G.M. (1989),** Effects of electrolytes, polymers and polyelectrolytes on particle deposition and detachment, *Colloid Surface* **39,** 107 - 126.

14. **Meinders, J.M., Van der Mei, H.C. and Busscher, H.J. (1994),** Physicochemical aspects of deposition of *Streptococcus thermophilus* B to hydrophobic and hydrophilic substrata in a parallel-plate flow chamber, *J Colloid Interf Sci* **164,** 355 - 363.

15. **Vadillo-Rodriguez, V., Busscher, H.J., Norde, W., De Vries, J. and Van der Mei, H.C. (2004),** Atomic force microscopic corroboration of bond aging for adhesion of *Streptococcus thermophilus* to solid substrata, *J Colloid Interf Sci* **278,** 251 - 254.

16. **Saravia-Otten, P., Muller, H.P. and Arvidson, S. (1997),** Transcription of *Staphylococcus aureus* fibronectin binding protein genes is negatively regulated by agr and an agr-independent mechanism, *J Bacteriol* **179,** 5259 - 5263.

17. **Busscher, H.J. and van der Mei, H.C. (2006),** Microbial adhesion in flow displacement systems, *Clin Microbiol Rev* **19,** 127 - 141.

18. **Camesano, T.A., Natan, M.J. and Logan, B.E. (2000),** Observation of changes in bacterial cell morphology using tapping mode atomic force microscopy, *Langmuir* **16,** 4563 - 4572.

19. **Cleveland, J.P., Manne, S., Bocek, D. and Hansma, P.K. (1993),** A nondestructive method for determining the spring constant of cantilevers for scanning force microscopy, *Rev Sci Instrum* **64,** 403 - 405.

20. **Nordmark, M.G., Laynez, J., Schon, A., Suurkuusk, J. and Wadso, I. (1984),** Design and testing of a new microcalorimetric vessel for use with living cellular-systems and in titration experiments, *J Biochem Biophys Method* **10,** 187 - 202.

21. **Wu, C.F., Chen, W.Y. and Lee, J.F. (1996),** Microcalorimetric studies of the interactions of imidazole with immobilized cu(ii): effects of pH value and salt concentration, *J Colloid Interf Sci* **183,** 236 - 242.

22. **Briggner, L.E. and Wadso, I. (1991),** Test and calibration processes for microcalorimeters, with special reference to heat-conduction instruments used with aqueous systems, *J Biochem Biophys Method* **22,** 101 - 118.

23. **Sousa, S.R., Manuela Bras, M., Moradas-Ferreira, P. and Barbosa, M.A. (2007),** Dynamics of fibronectin adsorption on TiO_2 surfaces, *Langmuir* **23,** 7046 - 7054.

24. **Haynes, C.A. and Norde, W. (1994),** Globular proteins at solid/liquid interfaces, *Colloid Surface B* **2,** 517 - 566.

25. **Moy, V.T., Florin, E.L. and Gaub, H.E. (1994),** Intermolecular forces and energies between ligands and receptors, *Science* **266,** 257 - 259.

26. **Mendez-Vilas, A., Gallardo-Moreno, A.M. and Gonzalez-Martin, M.L. (2006),** Nano-mechanical exploration of the surface and sub-surface of hydrated cells of *Staphylococcus epidermidis*, *Anton Leeuw Int J Gen Mol Microbiol* **89,** 373 - 386.

27. **Mendez-Vilas, A., Gallardo-Moreno, A.M., Calzado-Montero, R. and Gonzalez-Martin, M.L. (2008),** AFM probing in aqueous environment of *Staphylococcus epidermidis* cells naturally immobilised on glass: Physico-chemistry behind the successful immobilisation, *Colloid Surface B* **63,** 101 - 109.

28. **Xia, Z.M., Goldsmith, H.L. and Van de Ven, T.G.M. (1994),** Flow-induced detachment of red blood cells adhering to surfaces by specific antigen-antibody bonds, *Biophys J* **66,** 1222 - 1230.